QPSK

QUADRIPHASE-SHIFT KEYING

efficient utilization of channel bandwidth.

the phase of the carrier
$\pi/4$, $3\pi/4$, $5\pi/4$, and $7\pi/4$.

values we may define the transmitted signal as

$$s_i(t) = \begin{cases} \sqrt{\frac{2E}{T}} \cos\left[2\pi f_c t + (2i-1)\frac{\pi}{4}\right], & 0 \le t \le T \\ 0, & \text{elsewhere} \end{cases} \tag{6.23}$$

where $i = 1, 2, 3, 4$; E is the transmitted signal energy per symbol, and T is rhe symbol duration. The carrier frequency f_c equals n_c/T for some fixed integer n_c. Each possible value of the phase corresponds to a unique dibit. Thus, for example, we may choose the foregoing set of phase values to represent the *Gray-encoded* set of dibits: 10, 00, 01, and 11, where only a single bit is changed from one dibit to the next.

TABLE 6.1 *Signal-space characterization of QPSK*

Gray-encoded Input Dibit	*Phase of QPSK Signal (radians)*	*Coordinates of Message Points*	
		s_{i1}	s_{i2}
10	$\pi/4$	$+\sqrt{E/2}$	$-\sqrt{E/2}$
00	$3\pi/4$	$-\sqrt{E/2}$	$-\sqrt{E/2}$
01	$5\pi/4$	$-\sqrt{E/2}$	$+\sqrt{E/2}$
11	$7\pi/4$	$+\sqrt{E/2}$	$+\sqrt{E/2}$

Signal-Space Diagram of QPSK

Using a well-known trigonometric identity, we may use Equation (6.23) to redefine the transmitted signal $s_i(t)$ for the interval $0 \leq t \leq T$ in the equivalent form:

$$s_i(t) = \sqrt{\frac{2E}{T}} \cos\left[(2i - 1)\frac{\pi}{4}\right] \cos(2\pi f_c t) - \sqrt{\frac{2E}{T}} \sin\left[(2i - 1)\frac{\pi}{4}\right] \sin(2\pi f_c t) \quad (6.24)$$

where $i = 1, 2, 3, 4$. Based on this representation, we can make the following observations:

- There are two orthonormal basis functions, $\phi_1(t)$ and $\phi_2(t)$, contained in the expansion of $s_i(t)$. Specifically, $\phi_1(t)$ and $\phi_2(t)$ are defined by a pair of *quadrature carriers*:

$$\phi_1(t) = \sqrt{\frac{2}{T}} \cos(2\pi f_c t), \qquad 0 \leq t \leq T \quad (6.25)$$

$$\phi_2(t) = \sqrt{\frac{2}{T}} \sin(2\pi f_c t), \qquad 0 \leq t \leq T \quad (6.26)$$

- There are four message points, and the associated signal vectors are defined by

$$\mathbf{s}_i = \begin{bmatrix} \sqrt{E} \cos\left((2i - 1)\frac{\pi}{4}\right) \\ -\sqrt{E} \sin\left((2i - 1)\frac{\pi}{4}\right) \end{bmatrix}, \qquad i = 1, 2, 3, 4 \quad (6.27)$$

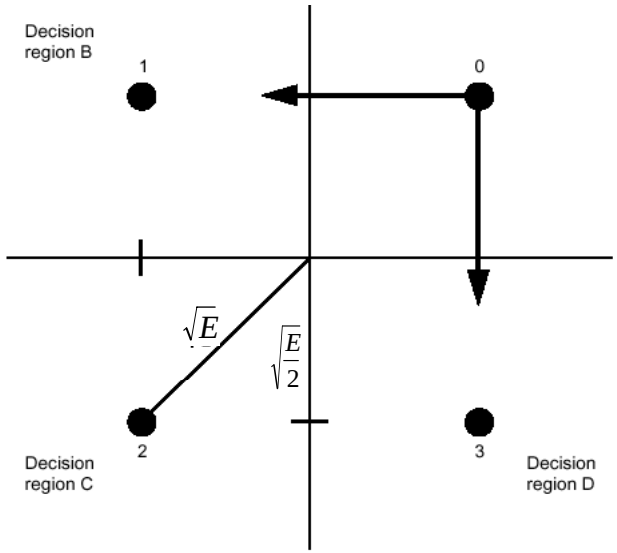

Figure 3.21 Necessary condition for an error to occur in a QPSK system.

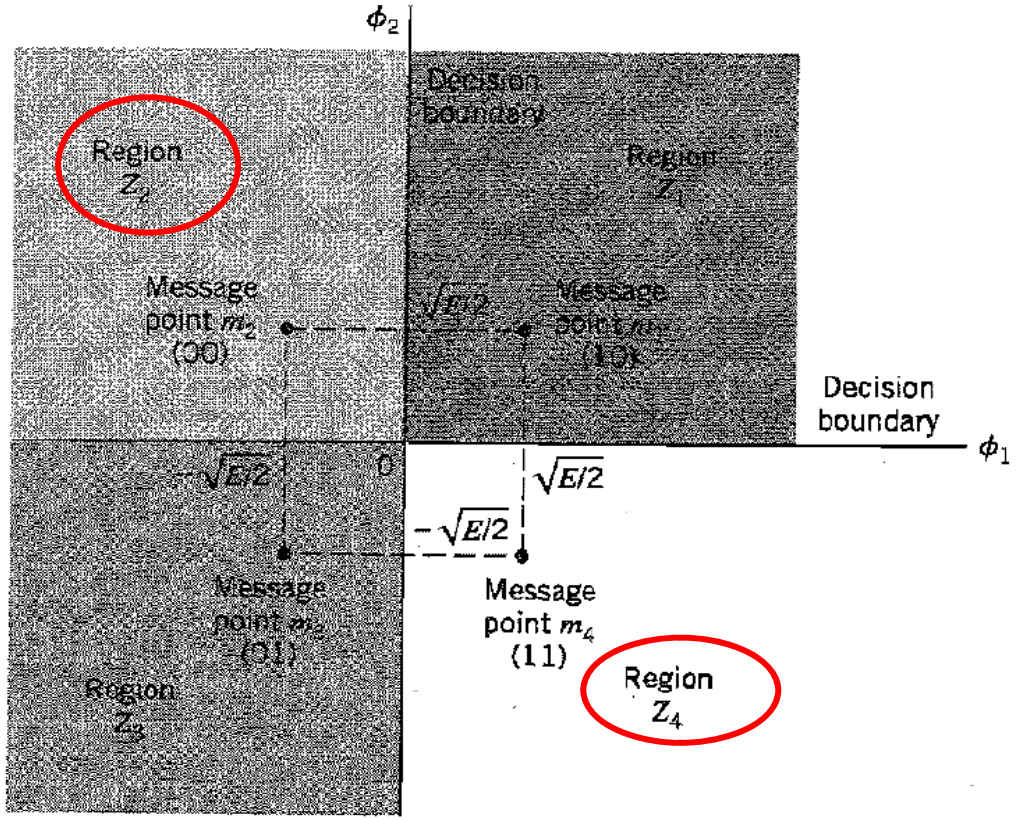

FIGURE 6.6 Signal-space diagram of coherent QPSK system.

TABLE 6.1 *Signal-space characterization of QPSK*

Gray-encoded Input Dibit	*Phase of QPSK Signal (radians)*	*Coordinates of Message Points*	
		s_{i1}	s_{i2}
10	$\pi/4$	$+\sqrt{E/2}$	$-\sqrt{E/2}$
00	$3\pi/4$	$-\sqrt{E/2}$	$-\sqrt{E/2}$
01	$5\pi/4$	$-\sqrt{E/2}$	$+\sqrt{E/2}$
11	$7\pi/4$	$+\sqrt{E/2}$	$+\sqrt{E/2}$

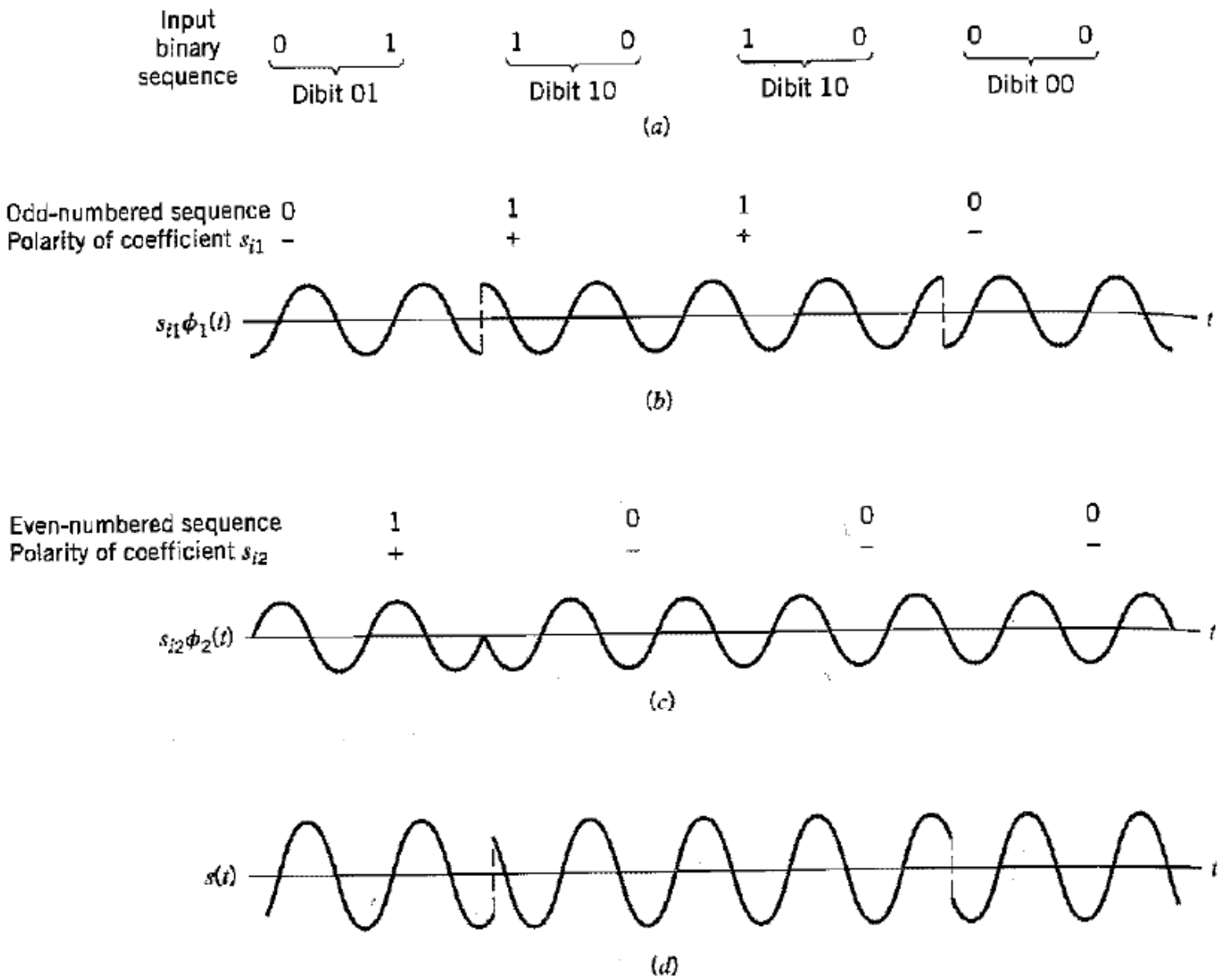

FIGURE 6.7 (*a*) Input binary sequence. (*b*) Odd-numbered bits of input sequence and associated binary PSK wave. (*c*) Even-numbered bits of input sequence and associated binary PSK wave. (*d*) QPSK waveform defined as $s(t) = s_{i1}\phi_1(t) + s_{i2}\phi_2(t)$.

Error Probability of QPSK

In a coherent QPSK system, the received signal $x(t)$ is defined by

$$x(t) = s_i(t) + w(t), \qquad \begin{cases} 0 \le t \le T \\ i = 1, 2, 3, 4 \end{cases} \tag{6.28}$$

where $w(t)$ is the sample function of a white Gaussian noise process of zero mean and power spectral density $N_0/2$. Correspondingly, the observation vector $\mathbf{x}$ has two elements, x_1 and x_2, defined by

$$\begin{aligned} x_1 &= \int_0^T x(t)\phi_1(t)\, dt \\ &= \sqrt{E}\cos\left[(2i-1)\frac{\pi}{4}\right] + w_1 \\ &= \pm\sqrt{\frac{E}{2}} + w_1 \end{aligned} \tag{6.29}$$

and

$$\begin{aligned} x_2 &= \int_0^T x(t)\phi_2(t)\, dt \\ &= -\sqrt{E}\sin\left[(2i-1)\frac{\pi}{4}\right] + w_2 \\ &= \mp\sqrt{\frac{E}{2}} + w_2 \end{aligned} \tag{6.30}$$

Thus the observable elements x_1 and x_2 are sample values of independent Gaussian random variables with mean values equal to $\pm\sqrt{E/2}$ and $\mp\sqrt{E/2}$, respectively, and with a common variance equal to $N_0/2$.

The decision rule is now simply to decide that $s_1(t)$ was transmitted if the received signal point associated with the observation vector $\mathbf{x}$ falls inside region Z_1, decide that $s_2(t)$ was transmitted if the received signal point falls inside region Z_2, and so on. An erroneous decision will be made if, for example, signal $s_4(t)$ is transmitted but the noise $w(t)$ is such that the received signal point falls outside region Z_4.

- The signal energy per bit is $E/2$.
- The noise spectral density is $N_0/2$.

Hence, using Equation (6.20) for the average probability of bit error of a coherent binary PSK system, we may now state that the average probability of bit error in *each* channel of the coherent QPSK system is

$$P' = \frac{1}{2}\operatorname{erfc}\left(\sqrt{\frac{E/2}{N_0}}\right) = \frac{1}{2}\operatorname{erfc}\left(\sqrt{\frac{E}{2N_0}}\right) \qquad (6.31)$$

$$Q\left(\sqrt{\frac{2E_b}{N_0}}\right)$$

$P[c|m_i] = (1-P_e)^2$

$P_{av}[\mathbf{e}] = \frac{1}{4}\left[4(1-2P_e+P_e^2)\right]$

$P_{av}[\xi] = 1 - P_{av}[c] = 2P_e - P_e^2$

$$P_c = (1-P')^2 = \left[1 - \frac{1}{2}\operatorname{erfc}\left(\sqrt{\frac{E}{2N_0}}\right)\right]^2 = 1 - \operatorname{erfc}\left(\sqrt{\frac{E}{2N_0}}\right) + \frac{1}{4}\operatorname{erfc}^2\left(\sqrt{\frac{E}{2N_0}}\right)$$

$P_e = Q\left[\frac{d}{\sqrt{2N_0}}\right] = Q\left[\sqrt{\frac{2E_b}{N_0}}\right]$

The average probability of symbol error for coherent QPSK is therefore

$$P_e = 1 - P_c = \operatorname{erfc}\left(\sqrt{\frac{E}{2N_0}}\right) - \frac{1}{4}\operatorname{erfc}^2\left(\sqrt{\frac{E}{2N_0}}\right) \qquad (6.33)$$

In the region where $(E/2N_0) \gg 1$, we may ignore the quadratic term on the right-hand side of Equation (6.33), so we approximate the formula for the average probability of symbol error for coherent QPSK as

$$P_e \approx \operatorname{erfc}\left(\sqrt{\frac{E}{2N_0}}\right) \qquad (6.34)$$

$$E = 2E_b \tag{6.36}$$

Thus expressing the average probability of symbol error in terms of the ratio E_b/N_0, we may write

$$P_e \simeq \operatorname{erfc}\left(\sqrt{\frac{E_b}{N_0}}\right) \tag{6.37}$$

With Gray encoding used for the incoming symbols, we find from Equations (6.31) and (6.36) that the *bit error rate* of QPSK is exactly

$$\text{BER} = \frac{1}{2}\operatorname{erfc}\left(\sqrt{\frac{E_b}{N_0}}\right) \qquad Q\left(\sqrt{\frac{2E_b}{N_0}}\right) \tag{6.38}$$

We may therefore state that a coherent QPSK system achieves the same average probability of bit error as a coherent binary PSK system for the same bit rate and the same E_b/N_0, but uses only half the channel bandwidth. Stated in a different way, for the same E_b/N_0 and therefore the same average probability of bit error, a coherent QPSK system transmits information at twice the bit rate of a coherent binary PSK system for the same channel bandwidth. For a prescribed performance, QPSK uses channel bandwidth better than binary PSK, which explains the preferred use of QPSK over binary PSK in practice.

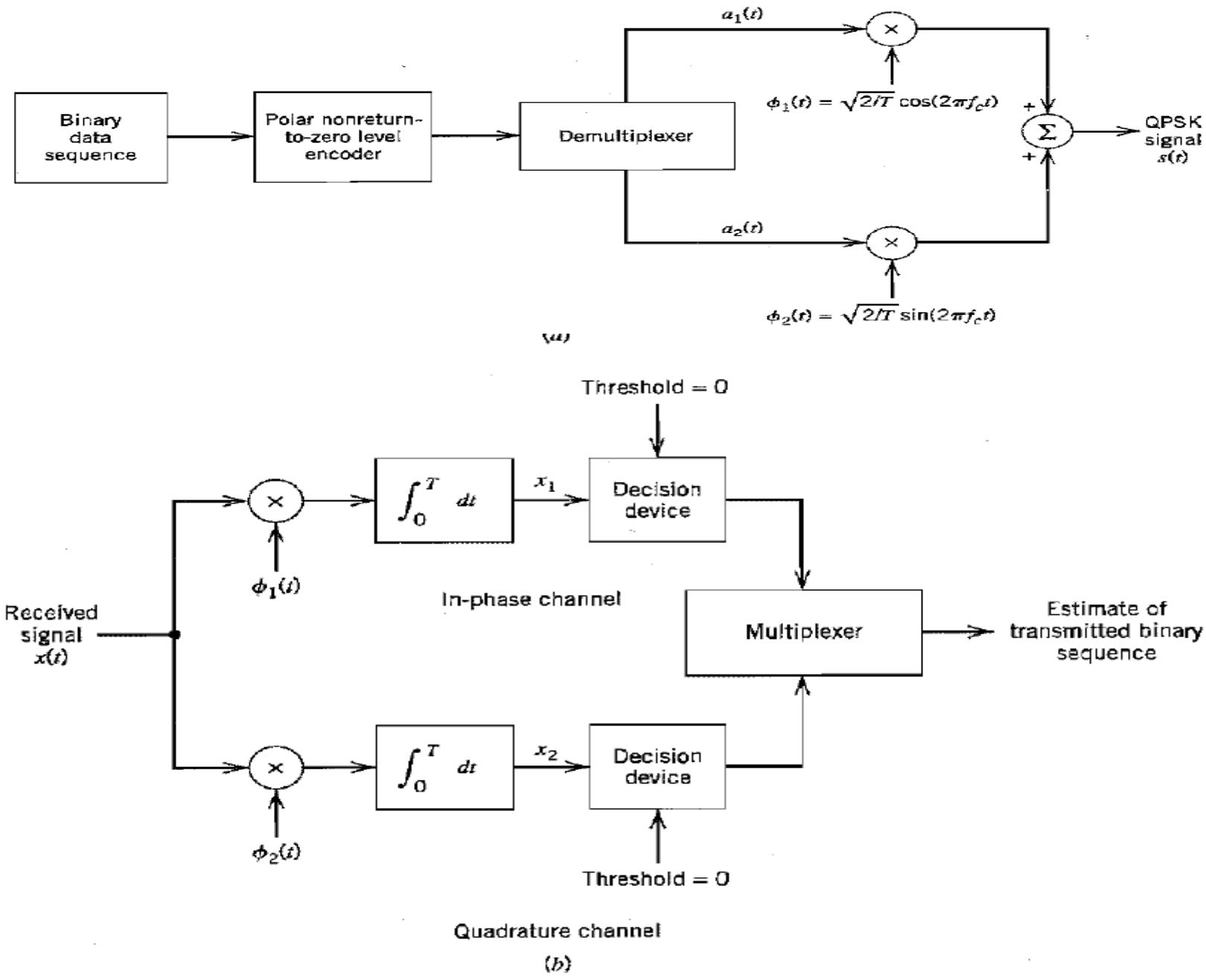

FIGURE 6.8 Block diagrams of (*a*) QPSK transmitter and (*b*) coherent QPSK receiver.

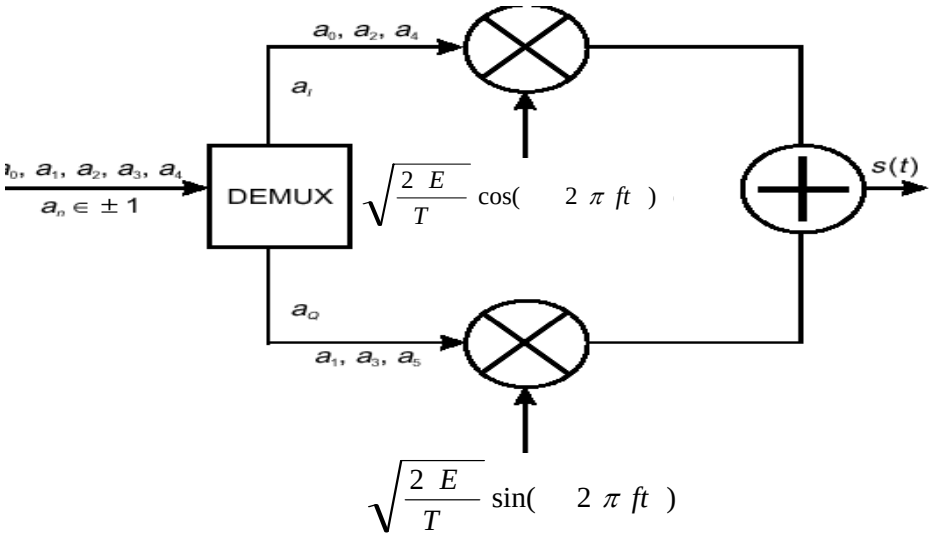

QPSK modulator.

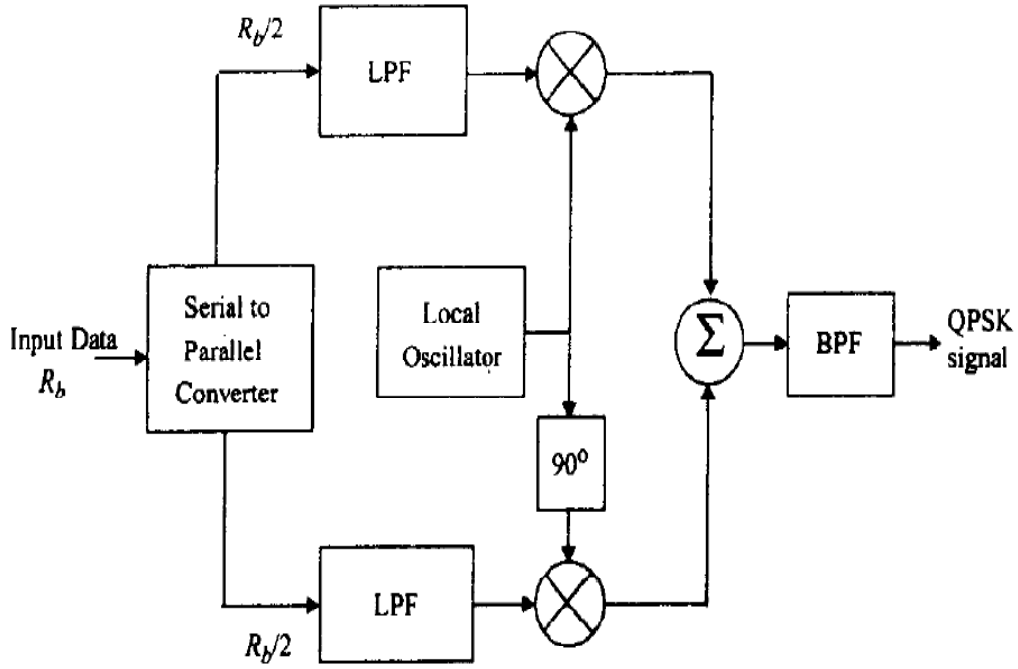

Figure 5.28
Block diagram of a QPSK transmitter.

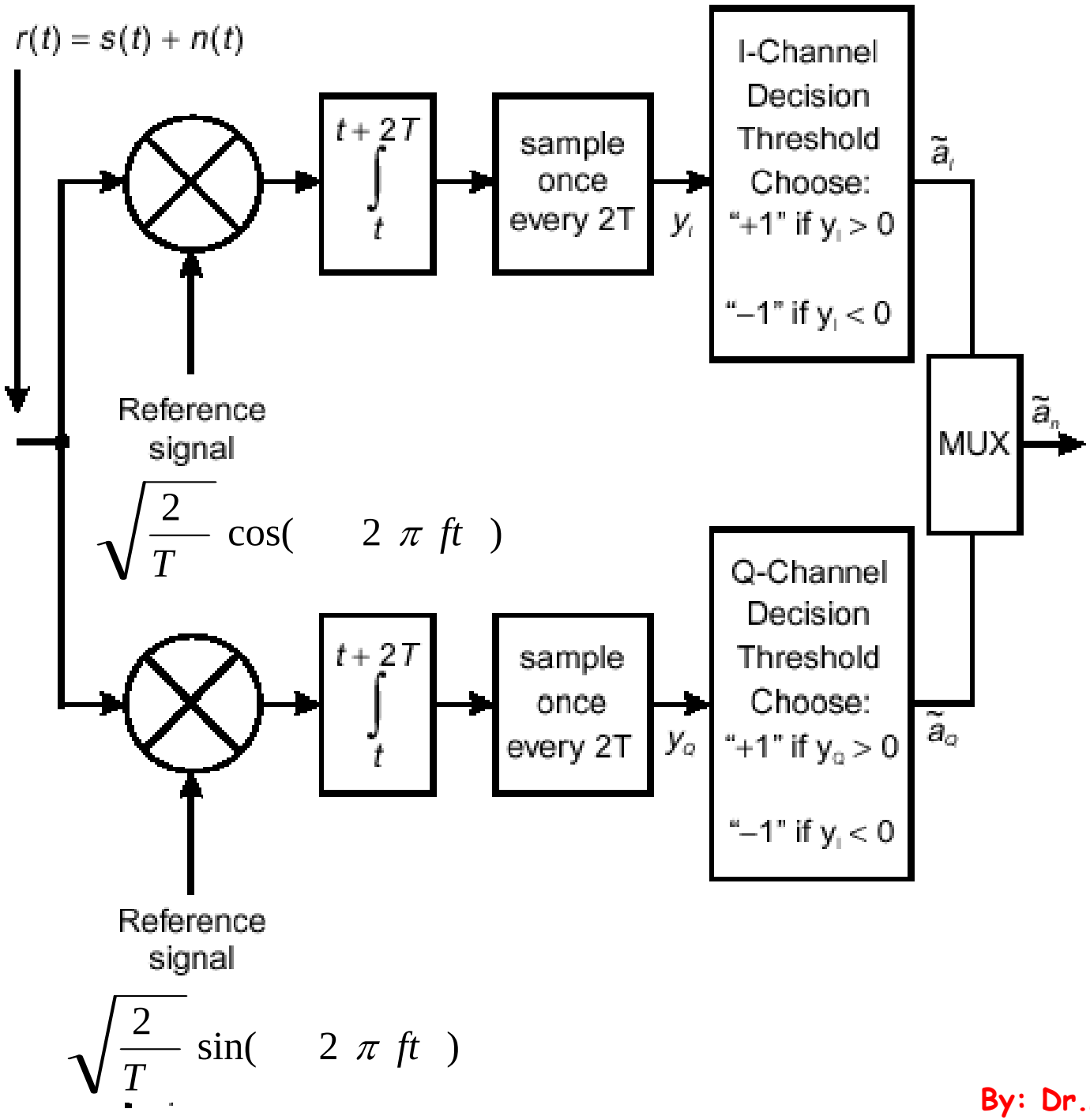

By: Dr.Mohab Mangoud

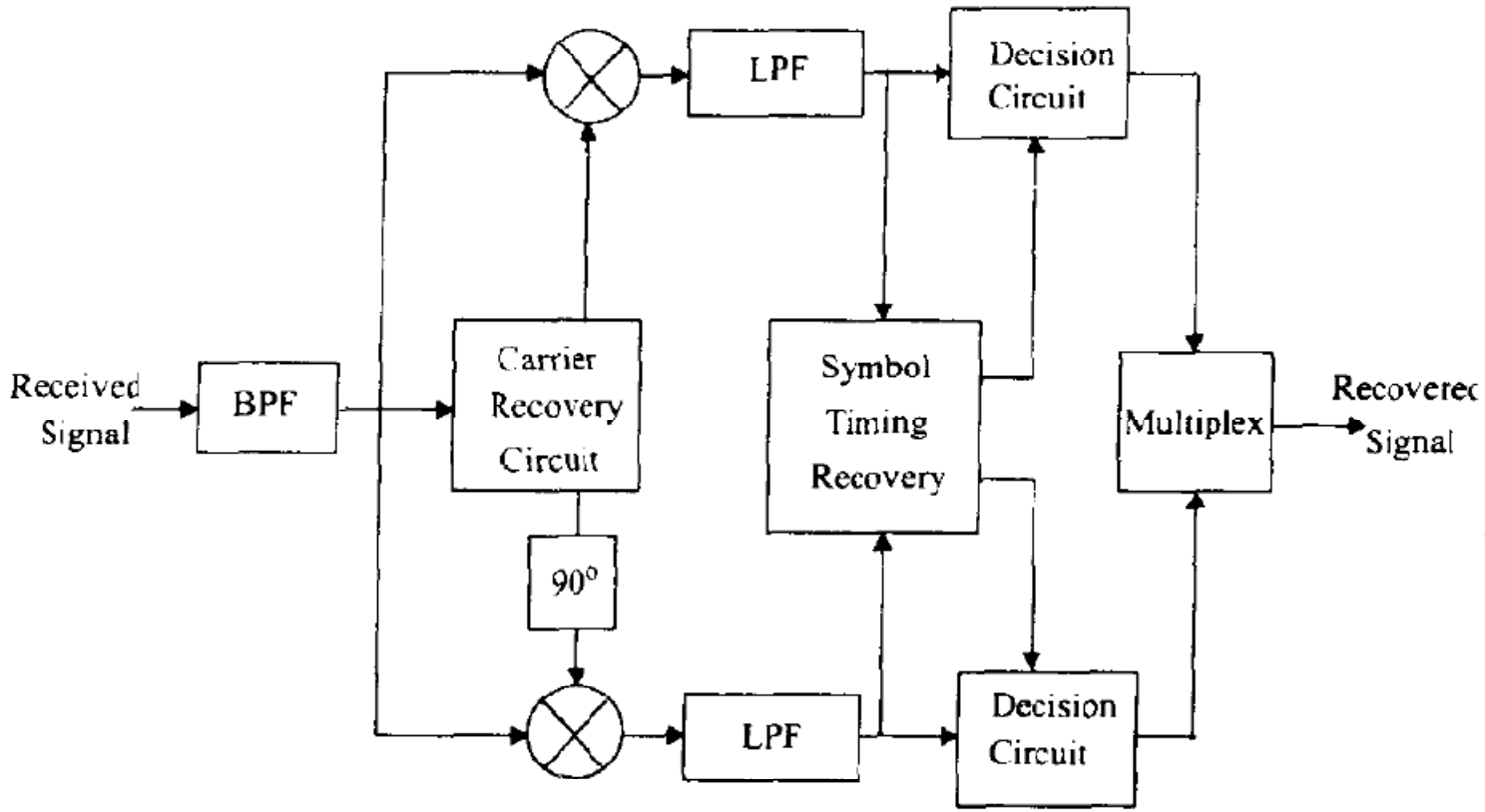

Figure 5.29
Block diagram of a QPSK receiver.

Power Spectra of QPSK Signals

Assume that the binary wave at the modulator input is random, with symbols 1 and 0 being equally likely, and with the symbols transmitted during adjacent time slots being statistically independent. We make the following observations pertaining to the in-phase and quadrature components of a QPSK signal:

1. Depending on the dibit sent during the signaling interval $-T_b \leq t \leq T_b$, the in-phase component equals $+g(t)$ or $-g(t)$, and similarly for the quadrature component. The $g(t)$ denotes the symbol shaping function, defined by

$$g(t) = \begin{cases} \sqrt{\frac{E}{T}}, & 0 \leq t \leq T \\ 0, & \text{otherwise} \end{cases} \tag{6.39}$$

   Hence, the in-phase and quadrature components have a common power spectral density, namely, $E\,\text{sinc}^2(Tf)$.

2. The in-phase and quadrature components are statistically independent. Accordingly, the baseband power spectral density of the QPSK signal equals the sum of the individual power spectral densities of the in-phase and quadrature components, so we may write

$$\begin{aligned} S_B(f) &= 2E\,\text{sinc}^2(Tf) \\ &= 4E_b\,\text{sinc}^2(2T_bf) \end{aligned} \tag{6.40}$$

Figure 6.9 plots $S_B(f)$, normalized with respect to $4E_b$, versus the normalized frequency fT_b. This figure also includes a plot of the baseband power spectral density of a certain form of binary FSK called minimum shift keying, the evaluation of which is presented in Section 6.5. Comparison of these two spectra is deferred to that section.

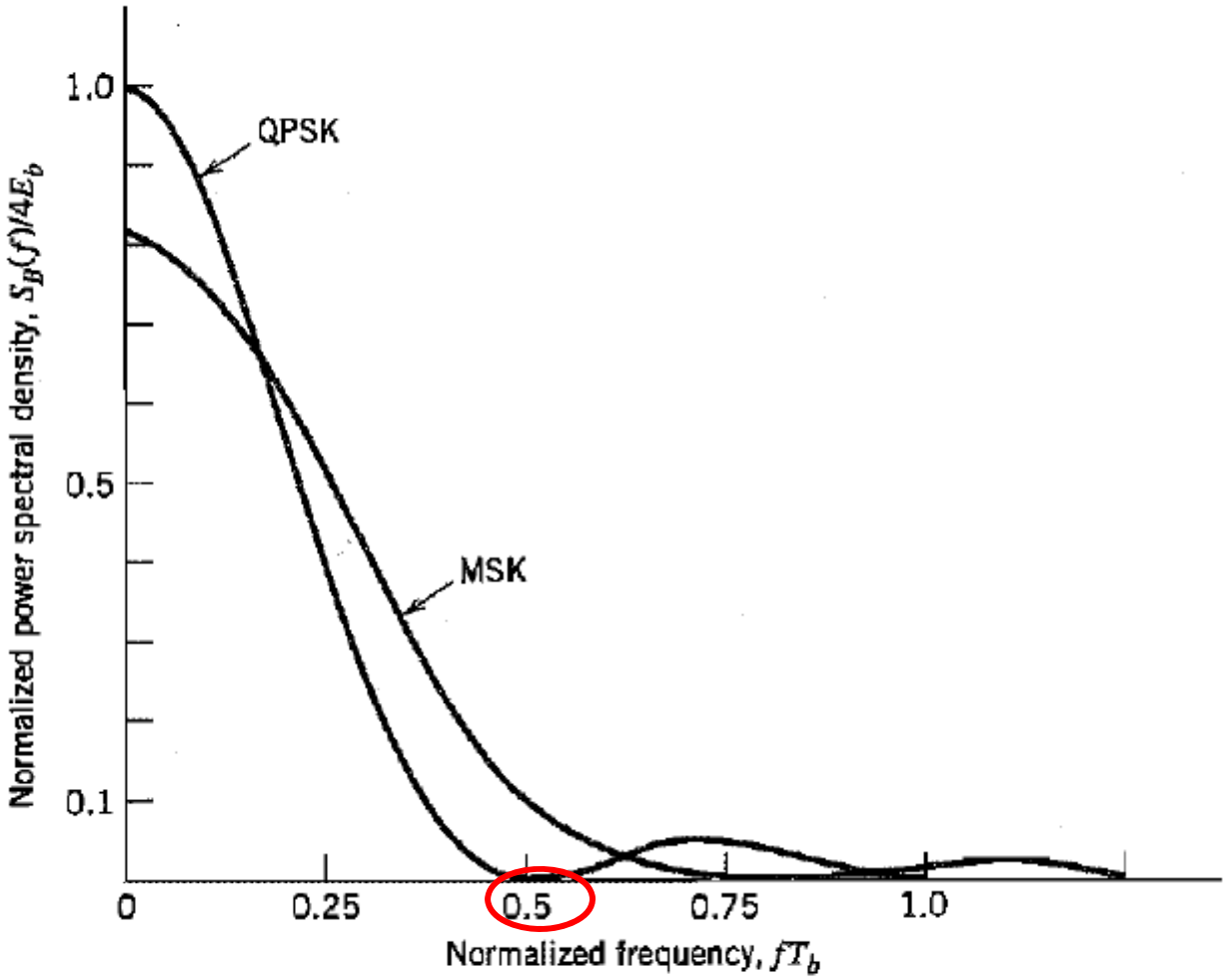

FIGURE 6.9 Power spectra of QPSK and MSK signals.

Rappaport

Spectrum and Bandwidth of QPSK Signals

The power spectral density of a QPSK signal can be obtained in a manner similar to that used for BPSK, with the bit periods T_b replaced by symbol periods T_s. Hence, the PSD of a QPSK signal using rectangular pulses can be expressed as

$$P_{QPSK} = \frac{E_s}{2}\left[\left(\frac{\sin\pi(f-f_c)T_s}{\pi(f-f_c)T_s}\right)^2 + \left(\frac{\sin\pi(-f-f_c)T_s}{\pi(-f-f_c)T_s}\right)^2\right] \tag{5.80}$$

$$= E_b\left[\left(\frac{\sin 2\pi(f-f_c)T_b}{2\pi(f-f_c)T_b}\right)^2 + \left(\frac{\sin 2\pi(-f-f_c)T_b}{2\pi(-f-f_c)T_b}\right)^2\right]$$

The PSD of a QPSK signal for rectangular and raised cosine filtered pulses is plotted in Figure 5.27. The null-to-null RF bandwidth is equal to the bit rate R_b, which is half that of a BPSK signal.

Rappaport

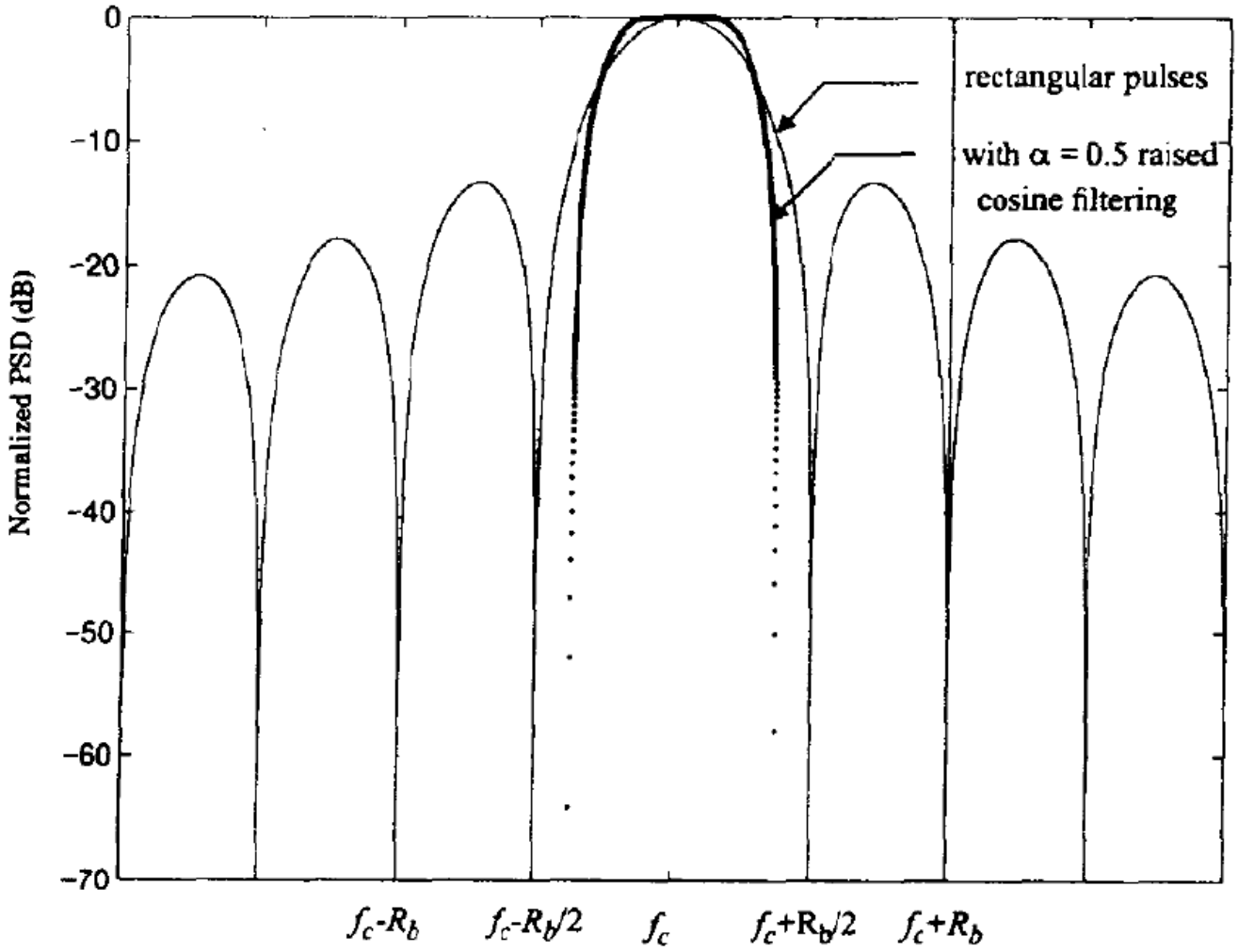

Figure 5.27
Power spectral density of a QPSK signal.

Based on this representation, a QPSK signal can be depicted using a two-dimensional constellation diagram with four points as shown in Figure 5.26a. It should be noted that different QPSK signal sets can be derived by simply rotating the constellation. As an example, Figure 5.26b shows another QPSK signal set where the phase values are $\pi/4$, $3\pi/4$, $3\pi/4$ and $7\pi/4$.

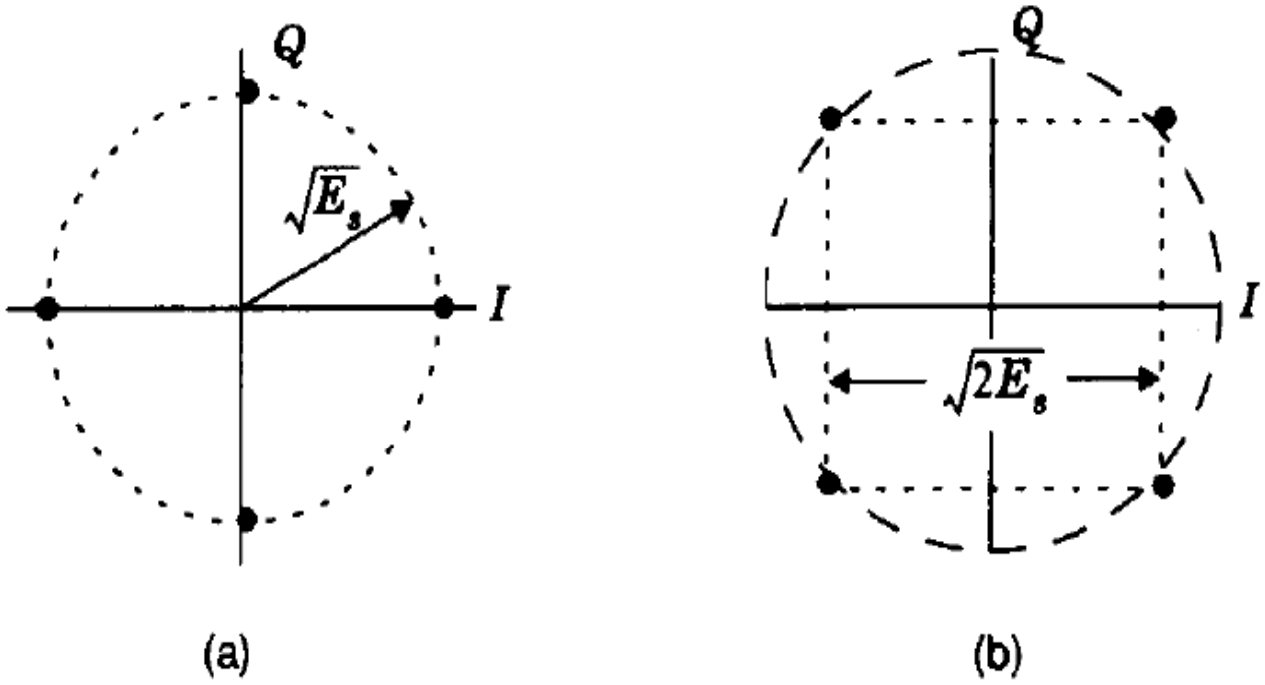

Figure 5.26

(a) QPSK constellation where the carrier phases are 0, $\pi/2$, π, $3\pi/2$.
(b) QPSK constellation where the carrier phases are $\pi/4$, $3\pi/4$, $5\pi/4$, $7\pi/4$.

OQPSK

5.7.5 Offset QPSK

The amplitude of a QPSK signal is ideally constant. However, when QPSK signals are pulse shaped, they lose the constant envelope property. The occasional phase shift of π radians can cause the signal envelope to pass through zero for just an instant. Any kind of hardlimiting or nonlinear amplification of the zero-crossings brings back the filtered sidelobes since the fidelity of the signal at small voltage levels is lost in transmission. To prevent the regeneration of sidelobes and spectral widening, it is imperative that QPSK signals be amplified only using linear amplifiers, which are less efficient. A modified form of QPSK, called *offset* QPSK (OQPSK) or *staggered* QPSK is less susceptible to these deleterious effects [Pas79] and supports more efficient amplification.

3.6.3 Applications in IS-95 CDMA System

The IS-95 CDMA system uses QPSK for both forward and reverse links. The reverse link, in particular, uses a variant of QPSK called *offset quadrature phase-shift keying* (OQPSK). OQPSK differs from the conventional QPSK in that prior to carrier multiplication, a delay of a half-bit interval (with respect to the I path) is placed in the Q path (see Figure 3.22). This is done to avoid a 180-degree phase transition that occurs in conventional QPSK systems. For example, when symbol 0 transitions to symbol 3, the signal goes through a 180-degree phase transition through the origin. In the time domain, the signal envelope collapses and momentarily reaches zero. This *zero crossing* demands a lot of dynamic range from the power amplifier. Thus, OQPSK is used on the reverse link where the power amplifier of the mobile is limited both in size and in performance. The extra delay of half a bit in the Q path ensures that there will be no direct transition between symbols 0 and 2 and between symbols 1 and 3, and thus no zero crossing.

It is also important to note that the error performance (i.e., probability of bit error) presented in this chapter is derived using an uncoded AWGN channel. In reality, error-correcting codes are used to improve the error

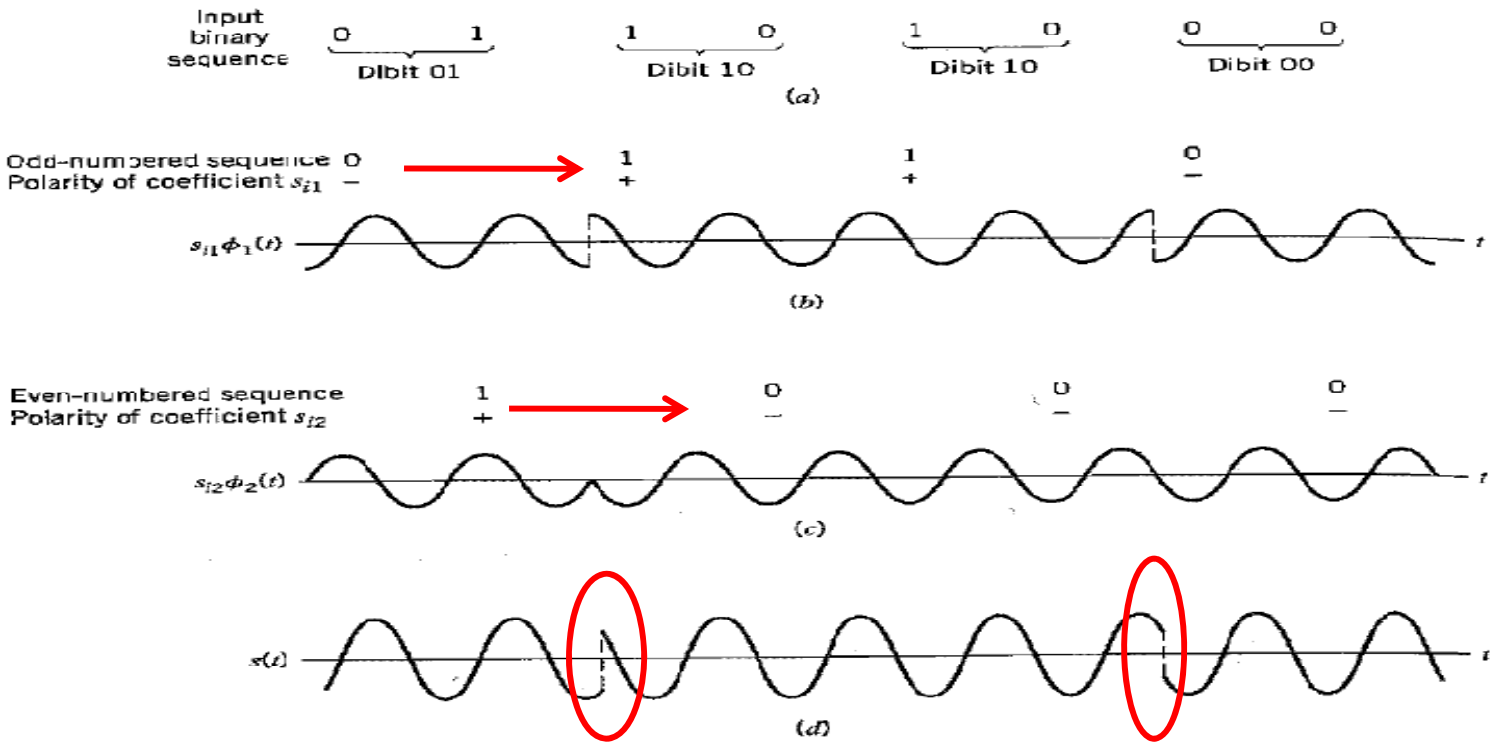

FIGURE 6.7 (*a*) Input binary sequence. (*b*) Odd-numbered bits of input sequence and associated binary PSK wave. (*c*) Even-numbered bits of input sequence and associated binary PSK wave.

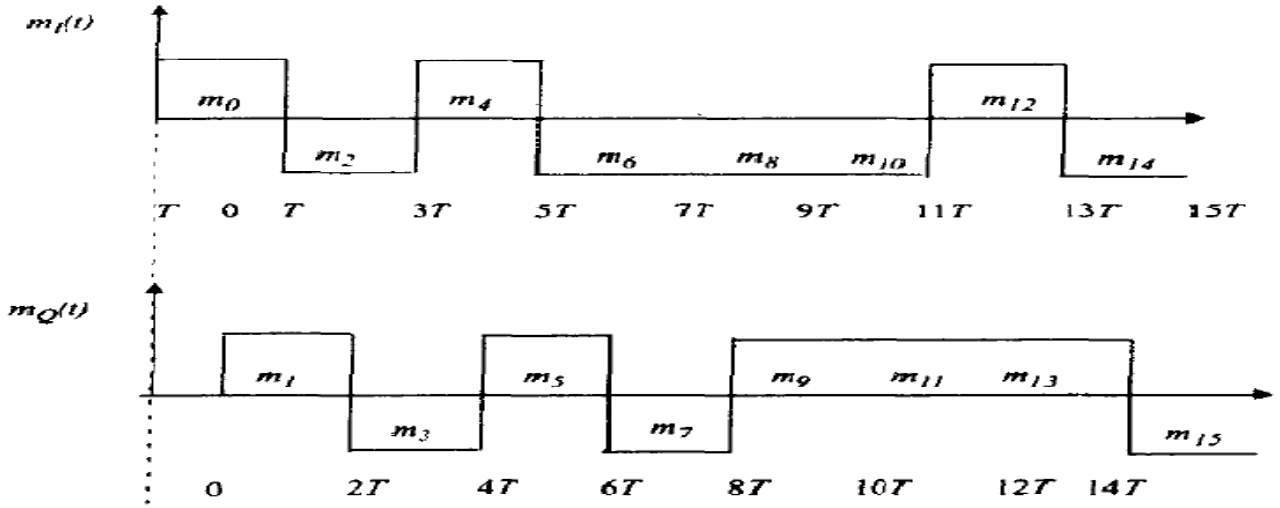

Figure 5.30
The time offset waveforms that are applied to the in-phase and quadrature arms of an OQPSK modulator. Notice that a half-symbol offset is used.

1. The carrier phase changes by ±180 degrees whenever both the in-phase and quadrature components of the QPSK signal changes sign. An example of this situation is illustrated in Figure 6.7 when the input binary sequence switches from dibit 01 to dibit 10.
2. The carrier phase changes by ±90 degrees whenever the in-phase or quadrature component changes sign. An example of this second situation is illustrated in Figure 6.7 when the input binary sequence switches from dibit 10 to dibit 00, during which the in-phase component changes sign, whereas the quadrature component is unchanged.
3. The carrier phase is unchanged when neither the in-phase component nor the quadrature component changes sign. This last situation is illustrated in Figure 6.7 when dibit 10 is transmitted in two successive symbol intervals.

Situation 1 and, to a much lesser extent, situation 2 can be of a particular concern when the QPSK signal is filtered during the course of transmission, prior to detection. Specifically, the 180- and 90-degree shifts in carrier phase can result in changes in the carrier amplitude (i.e., envelope of the QPSK signal), thereby causing additional symbol errors on detection.

The extent of amplitude fluctuations exhibited by QPSK signals may be reduced by using *offset QPSK*.[2] In this variant of QPSK, the bit stream responsible for generating the quadrature component is delayed (i.e., offset) by half a symbol interval with respect to the bit stream responsible for generating the in-phase component. Specifically, the two basis functions of offset QPSK are defined by

$$\phi_1(t) = \sqrt{\frac{2}{T}}\cos(2\pi f_c t), \qquad 0 \le t \le T \tag{6.41}$$

$$\phi_2(t) = \sqrt{\frac{2}{T}}\sin(2\pi f_c t), \qquad \frac{T}{2} \le t \le \frac{3T}{2} \tag{6.42}$$

Accordingly, unlike QPSK, the phase transitions likely to occur in offset QPSK are confined to ±90 degrees, as indicated in the signal space diagram of Figure 6.10*b*. However, ±90 degree phase transitions in offset QPSK occur twice as frequently but with half the intensity encountered in QPSK. Since, in addition to ±90-degree phase transitions, ±180-degree phase transitions also occur in QPSK, we find that amplitude fluctuations in offset QPSK due to filtering have a smaller amplitude than in the case of QPSK.

Despite the delay $T/2$ applied to the basis function $\phi_2(t)$ in Equation (6.42) compared to that in Equation (6.26), the offset QPSK has exactly the same probability of symbol error in an AWGN channel as QPSK.

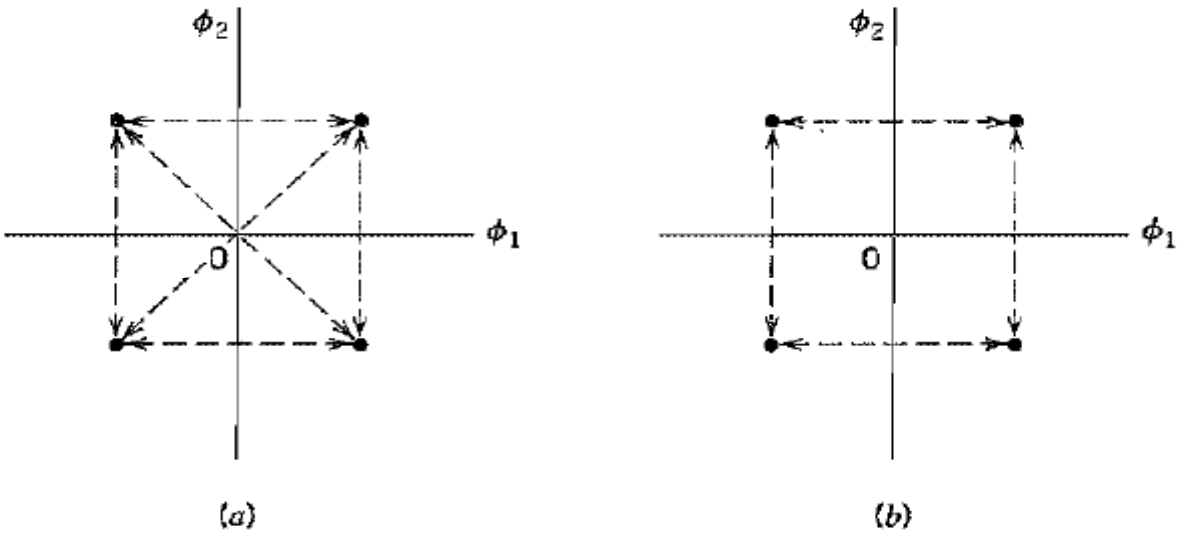

FIGURE 6.10 Possible paths for switching between the message points in (*a*) QPSK and (*b*) offset QPSK.

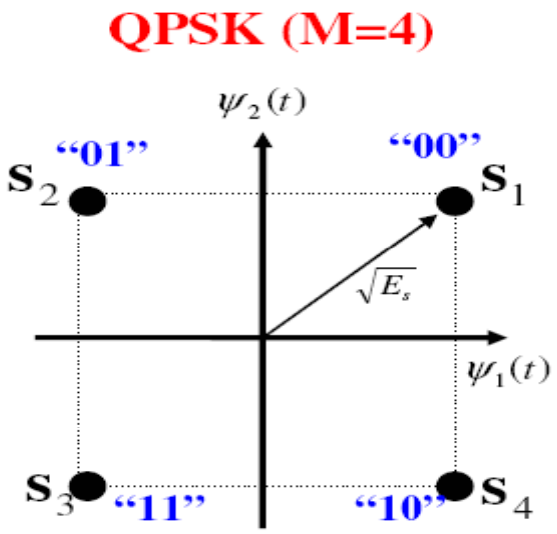

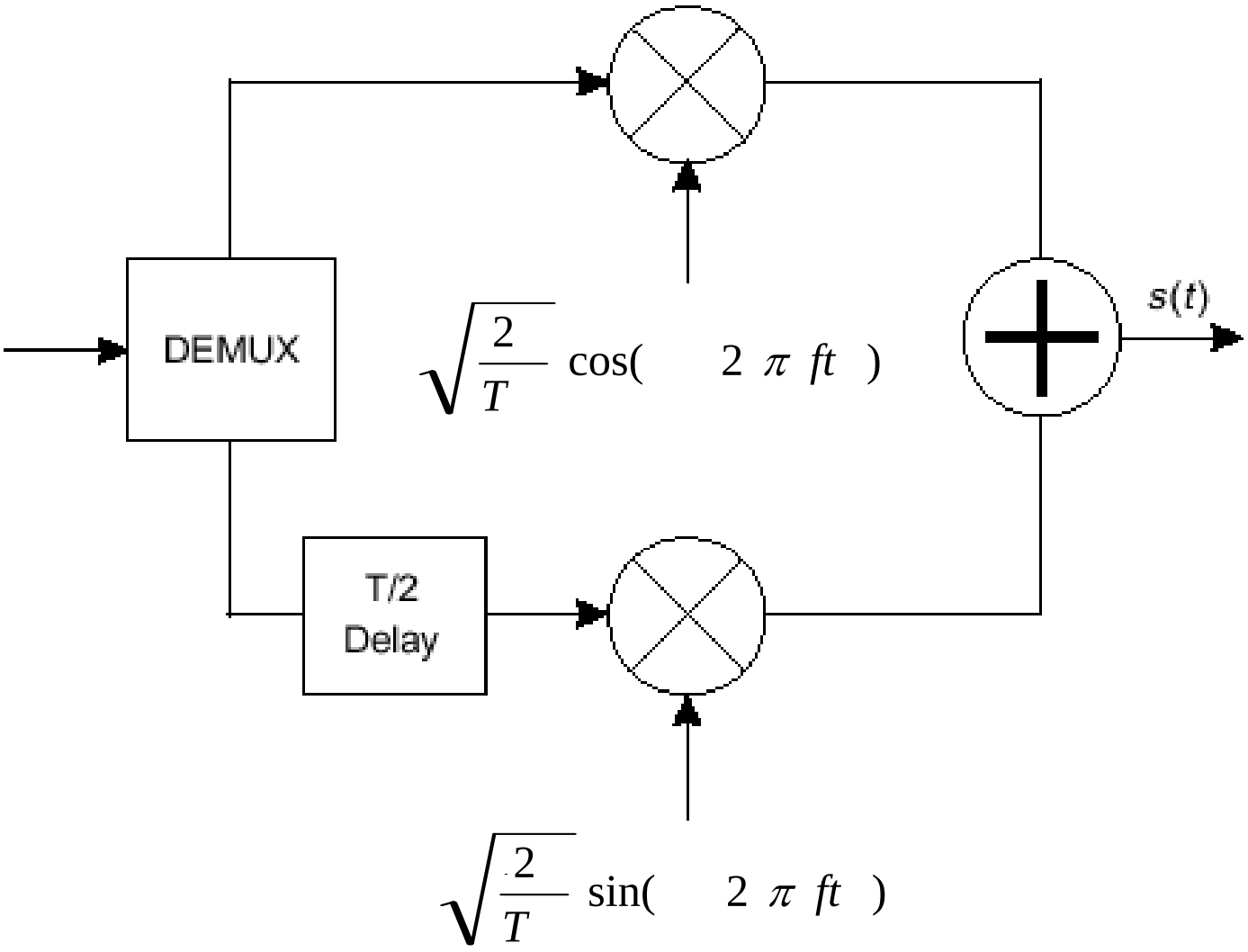

Figure 3.22 OQPSK modulator.

$\pi/4$ shifted QPSK

$\pi/4$-SHIFTED QPSK

An ordinary QPSK signal may reside in either one of the two commonly used constellations shown in Figures 6.11*a* and 6.11*b*, which are shifted by $\pi/4$ radians with respect to each other. In another variant of QPSK known as *$\pi/4$-shifted QPSK*,[3] the carrier phase used for the transmission of successive symbols (i.e., dibits) is alternately picked from one of the two QPSK constellations in Figure 6.11 and then the other. It follows therefore that a $\pi/4$-shifted QPSK signal may reside in any one of eight possible phase states, as indicated

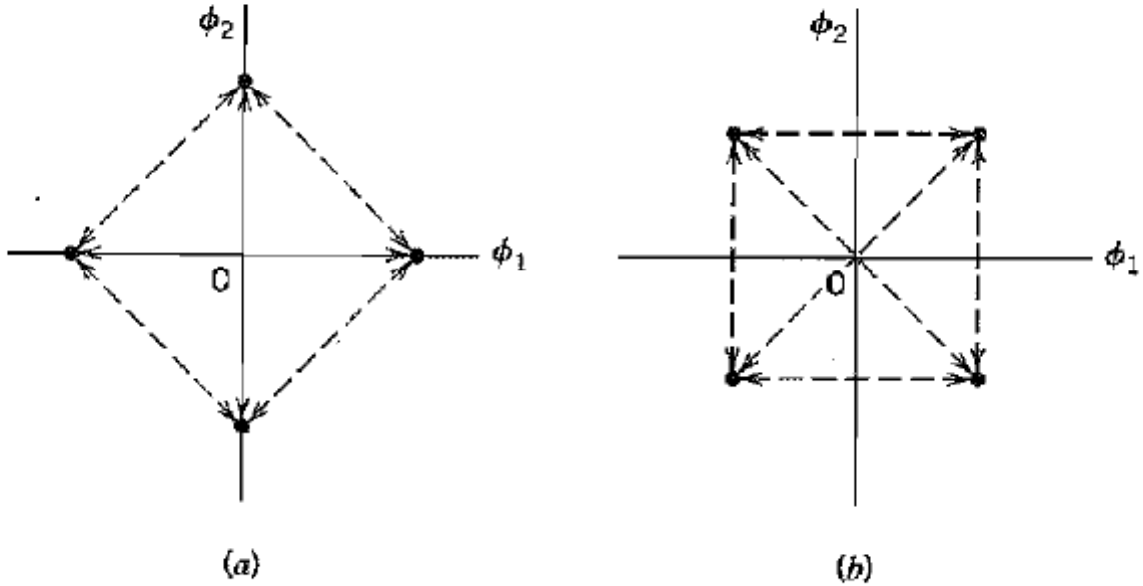

FIGURE 6.11 Two commonly used signal constellations for QPSK; the arrows indicate the paths along which the QPSK modulator can change its state.

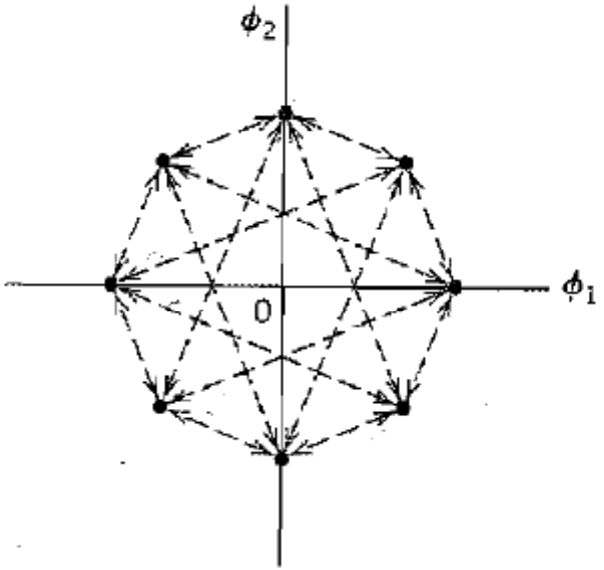

FIGURE 6.12 Eight possible phase states for the $\pi/4$-shifted QPSK modulator.

TABLE 6.2 ***Correspondence between input dibit and phase change for $\pi/4$-shifted DQPSK***

Gray-Encoded Input Dibit	*Phase Change, $\Delta\theta$ (radians)*
00	$\pi/4$
01	$3\pi/4$
11	$-3\pi/4$
10	$-\pi/4$

in Figure 6.12. The four dashed lines emanating from each possible message point in Figure 6.12 define the phase transitions that are feasible in $\pi/4$-shifted QPSK.

Table 6.2 summarizes a possible set of relationships between the phase transitions in this new digital modulation scheme and the incoming Gray-encoded dibits. For example, if the modulator is in one of the phase states portrayed in Figure 6.11*b*, then on receiving the dibit 00 it shifts into a phase state portrayed in Figure 6.11*a* by rotating through $\pi/4$ radians in a counterclockwise direction.

Attractive features of the $\pi/4$-shifted QPSK scheme include the following:

- The phase transitions from one symbol to the next are restricted to $\pm\pi/4$ and $\pm 3\pi/4$ radians, which is to be contrasted with the $\pm\pi/2$ and $\pm\pi$ phase transitions in QPSK. Consequently, envelope variations of $\pi/4$-shifted QPSK signals due to filtering are significantly reduced, compared to those in QPSK.
- Unlike offset QPSK signals, $\pi/4$-shifted QPSK signals can be noncoherently detected, thereby considerably simplifying the receiver design. Moreover, like QPSK signals, $\pi/4$-shifted QPSK can be differently encoded,